

# Performance of the Unified Readout System of Belle II

Mikihiko Nakao, Ryosuke Itoh, Satoru Yamada, Soh Y. Suzuki, Tomoyuki Konno, Qi-Dong Zhou, Takuto Kunigo, Ryohei Sugiura, Seokhee Park, Zhen-An Liu, Jingzhou Zhao, Igor Konorov, Dmytro Levit, Katsuro Nakamura, Hikaru Tanigawa, Nanae Taniguchi, Tomohisa Uchida, Kurtis Nishimura, Oskar Hartbrich, Yun-Tsung Lai, Masayoshi Shoji, Alexander Kuzmin, Vladimir Zhulanov, Brandon Kunkler, Isar Mostafanezhad, Hideyuki Nakazawa, and Yuji Unno

**Abstract**—Belle II experiment at the SuperKEKB collider at KEK, Tsukuba, Japan has successfully started the data taking with the full detector in March 2019. Belle II is a luminosity frontier experiment of the new generation to search for physics beyond the Standard Model of elementary particles, from precision measurements of a huge number of  $B$  and charm mesons and tau leptons. In order to read out the events at a high rate from the seven subdetectors of Belle II, we adopt a highly unified readout system, including a unified trigger timing distribution system (TTD), a unified high speed data link system (Belle2link), and a common backend system to receive Belle2link data. Each subdetector frontend readout system has a field-programmable gate array (FPGA) in which unified firmware components of the TTD receiver and Belle2link transmitter are embedded. The system is designed for data taking at a trigger rate up to 30 kHz with a dead-time fraction of about 1% in the frontend readout system. The trigger rate during the nominal operation is still much lower than our design. However, the background level is already high due to the initial vacuum condition and other accelerator parameters, and it is the most limiting factor of the accelerator and detector operation. Hence the occupancy and the stress to the frontend electronics are rather severe, and they cause various kind of instabilities. We present the performance of the system, including the achieved trigger rate, dead-time fraction, stability, and discuss the experiences gained during the operation.

**Index Terms**—Availability, Centralized control, Data acquisition, Data transfer, High energy physics, Radiation effects, System integration, Synchronization

Manuscript received Month XX, 2020.

M. Nakao (e-mail: mikihiko.nakao@kek.jp), R. Itoh, S.Y. Suzuki, K. Nakamura are with KEK, High Energy Accelerator Research Organization, and SOKENDAI, the Graduate University for Advanced Studies, Tsukuba, 305-0801 Japan.

S. Yamada, T. Kunigo, S. Park, N. Taniguchi, T. Uchida, and M. Shoji are with KEK, High Energy Accelerator Research Organization, Tsukuba, 305-0801 Japan.

T. Konno is with Kitasato University, Sagamihara, 252-0373 Japan.

Q.D. Zhou is with Nagoya University, Nagoya, 464-8602 Japan.

R. Sugiura and H. Tanigawa are with Tokyo University, Tokyo, 113-0033 Japan.

Z.-A. Liu and J. Zhao are with Institute of High Energy Physics, Chinese Academy of Sciences, Beijing, 100049 China

I. Konorov and D. Levit are with Technische Universität München, Garching, 85748 Germany

K. Nishimura, O. Hartbrich and I. Mostafanezhad are with University of Hawaii, Honolulu, 96822 USA.

Y.-T. Lai is with Kavli Institute for the Physics and Mathematics of the Universe, University of Tokyo, Kashiwa, 277-8583 Japan.

A. Kuzmin and V. Zhulanov are with Budker Institute of Nuclear Physics SB RAS, Novosibirsk, 630090 Russia.

B. Kunkler is with Indiana University, Bloomington, 47408 USA.

H. Nakazawa is with National Taiwan University, Taipei, 10617 Taiwan.

Y. Unno is with Hanyang University, Seoul, 04763 Korea.

## I. INTRODUCTION

Belle II experiment [1] at the SuperKEKB  $e^+e^-$  collider [2] at KEK, Tsukuba, Japan has successfully started the data taking to play the role of the new generation luminosity frontier experiment to search for physics beyond the Standard Model of elementary particles. The goal of the Belle II experiment is to collect unprecedented  $50 \text{ ab}^{-1}$  integrated luminosity mostly at the  $\Upsilon(4S)$  resonance, to study and search for a wide range of  $B$  meson decays, charm meson decays,  $\tau$  lepton decays, and hypothetical particles such as those expected from the dark sector. The design instantaneous luminosity is  $8 \times 10^{35} \text{ cm}^{-2}\text{s}^{-1}$ , 40 times higher than the highest luminosity achieved by its predecessor, KEKB. Thanks to the clean environment of the  $e^+e^-$  collision, the events are triggered with a single level (level-1) trigger system with a trigger efficiency greater than 99% for most of the  $B$  meson decay modes. The level-1 trigger rate is designed to be up to 30 kHz, which includes about 1 kHz each of  $B$ -meson-pair, charm-pair, and  $\tau$ -lepton-pair events.

The Belle II detector consists of seven subdetectors: a pixel detector (PXD) and a silicon-strip vertex detector (SVD) for vertex reconstruction, a central drift chamber (CDC) for charged track reconstruction, a time-of-propagation counter (TOP) and an aerogel rich counter (ARICH) for charged hadron identification, an electromagnetic calorimeter (ECL) for photon detection and electron identification, and a  $K_L$  and muon detector (KLM) in the return yoke of the 1.5 T solenoid coil. The event is read out upon each level-1 trigger decision based mostly on CDC and ECL trigger information which is given within a latency of about  $5 \mu\text{s}$ . All the detector data are digitized inside or nearby the detector, and collected by the data acquisition system.

The first physics run was in 2018 with the Belle II detector without the vertex detectors, under the so-called “phase 2” operation. The main purposes were the commissioning of the accelerator, evaluation of the background condition for the vertex detectors, and initial physics programs with a low-multiplicity trigger condition and with no requirement on the precise vertex information. The main physics program, so-called “phase 3”, has successfully started in 2019 with the full Belle II detector. Although the luminosity is still far below the design, it reached the peak luminosity of  $2.4 \times 10^{34} \text{ cm}^{-2}\text{s}^{-1}$ , already exceeding the previous record established by KEKB.

Belle II has collected  $74 \text{ fb}^{-1}$  of data, with an overall efficiency of about 84% as discussed later.

In this paper, we first briefly describe the unified readout system of Belle II, and then the performance of the system and various troubles we experienced in the first two years of the operation.

## II. UNIFIED READOUT SYSTEM

In order to read out the events from the seven subdetectors, we adopt a highly unified readout system [3] [4], including a unified trigger timing distribution (TTD) system for the entire Belle II detector, a unified high speed data link system called “Belle2link” which is used by all subdetectors except PXD, and a common backend system called “COPPER” to receive the Belle2link data. Every subdetector frontend electronics (FEE) device has an FPGA in which the unified firmware components of TTD receiver and Belle2link transmitter are embedded.

The system aims for taking data at 30 kHz trigger rate with a dead-time fraction of about 1% from the frontend readout system. The read-out data are sent to the backend data acquisition system comprised of the event builder, high level trigger and storage system. The schematic view of the Belle data acquisition system is given in Fig. 1.

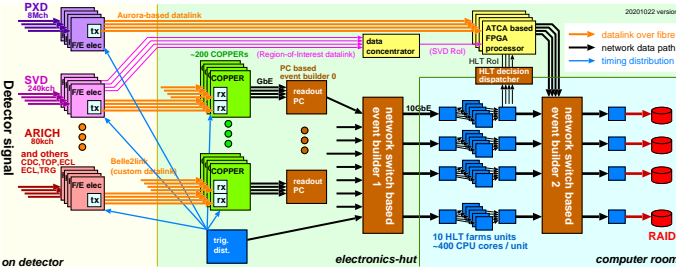


Fig. 1. Schematic view of the Belle II data acquisition system.

### A. Unified Trigger Timing Distribution

The TTD system is a tree-like connection of the frontend-timing-switch (FTSW) modules to a large number of FEE boards and COPPER modules, to distribute the system clock, level-1 trigger timing and other information for fast control and to collect the status of FEE and COPPER [5]. The system clock of 127 MHz is generated from the 509 MHz radio frequency (RF) of SuperKEKB, and is directly distributed using a dedicated line. The remaining signals are embedded in a bidirectional serial link of 254 Mbps using a custom protocol called “b2tt.” These signals are transmitted as low voltage differential signaling (LVDS) signals over a category-7 network cable for most of the connections, or over two pairs of multimode fibers for the connections between the stations on the detector and the electronics-hut where the center of the TTD system resides.

The FTSW module [5] is a multi-purpose double-width 6U-height VMEbus [6] module equipped with a Xilinx [7] Virtex-5 FPGA and 24 RJ-45 connectors. Four of these connectors have dedicated purposes: one for the connection to uplink, one

for programming of the FPGA of the FTSW using JTAG [8], one for Ethernet (unused), and one for multipurpose LVDS input or output; and remaining 20 connectors are used for distribution. The bottom 4 or 8 distribution RJ-45 connectors can be replaced with an FMC daughter card with 2- or 8-port SFP optical transceivers, to receive or distribute the b2tt serial-link signals. Up to 4 stages of cascaded connections of FTSW modules are used to deliver the TTD signal to more than 1,000 destinations of FEE boards and other systems as shown in Fig. 2.

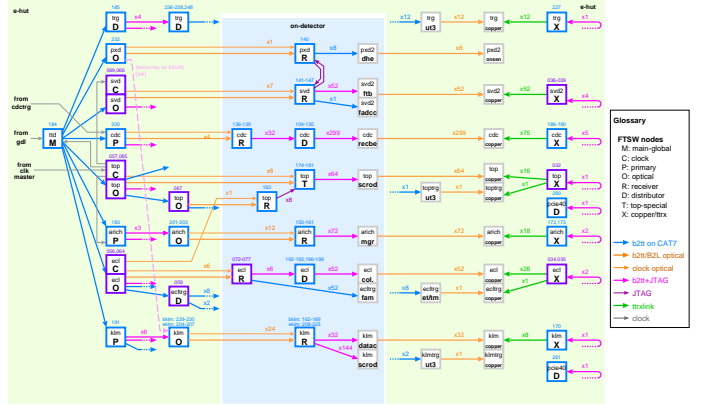


Fig. 2. Schematic view of the trigger timing distribution tree. The symbols M, C, O, P, R, D, T, X correspond to different firmware used by FTSW modules.

The FTSW module is also used to deliver the JTAG signals to the frontend boards, first encoded in the b2tt protocol and delivered to the last step of the FTSW tree, and then transmitted as LVDS level signals to the FEE over another category-7 cable. Therefore, a typical FTSW module on the detector is receiving the b2tt serial link over 2 pairs of fibers and connected with 8 FEE boards for timing distribution and JTAG programming.

The TTD system distributes the level-1 trigger signal with the event number, timestamp and trigger type. The timestamp is a unique and always incremented 59-bit value for every event, and it is saved in the data to be used later to detect the event mismatch and data error at various stages of the readout chain. The trigger type is used to dynamically change the readout operation of FEE depending on the trigger source. The trigger interval is controlled by a programmable interval counter and an emulation logic of the SVD FEE to avoid the overflow in the SVD FEE, which has the most timing-critical condition among subdetectors. In addition, busy signals are accepted to pose the back pressure from the backend data transport and some of the FEE systems.

At the same time, the TTD tree is used to collect and summarize the status of the readout system, including error information, number of processed events, and status of the SEU mitigation (see section IV-A). Each connection can be masked or reset remotely, to avoid spurious information from unused or malfunctioning links. In addition to the FEE, the TTD system also distributes various fast timing information to subdetector and global trigger processors, luminosity counters, and beam background monitors.

## B. Unified Data Link — Belle2link

The Belle2link is a bi-directional custom high-speed serial link protocol to collect the data read out at the FEE [9]. It uses the 8b10b encoded GTP or GTX high speed serial link function of the Xilinx FPGA. The raw bit rate is 2.54 Gbps, driven by the system clock, but the payload bandwidth is limited to about 1 Gbps at the FEE, mainly because the bandwidth is limited at the COPPER backend and there is no back pressure from the COPPER to the FEE.

The receiver of the Belle2link is a single-channel optical receiver card called “HSLB,” which equips a Xilinx Virtex-5 FPGA. Up to 4 HSLB cards are mounted on a COPPER module, which is a 9U-height VMEbus board. The COPPER module is driven by a processor card running Linux operating system on a Intel x86 processor. The COPPER module is a multi-purpose platform which is also used by other experiments with different daughter cards instead of the HSLB.

The event fragment data sent from the FEE is checked for error, and then copied to the FIFO buffer of the COPPER. The COPPER module then combines the event fragments and make a direct memory access (DMA) transfer to the processor. The processor is used to make a minimal formatting and send the data to the next stage through a Gigabit Ethernet connection.

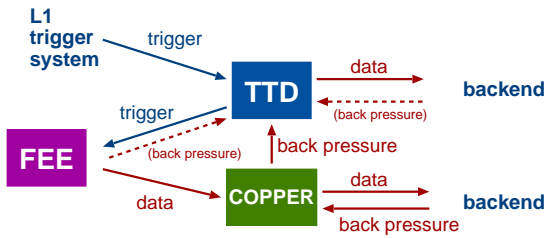


Fig. 3. Trigger, data, and back-pressure paths of the unified readout system.

The COPPER board also equips a trigger card for the connection to the TTD system. A programmable threshold is set to the FIFO buffer, and when the data exceeds the threshold, a back pressure is sent to the TTD system. The entire path of the trigger distribution, data collection, and back pressure is illustrated in Fig. 3.

The HSLB card also serves as interface to the FEE, to make a read and write access to the 32-bit registers mapped onto a 16-bit address space. These registers are used to configure individual boards, such as setting the threshold or parameters that are needed for feature extraction from the read-out signal waveform, and reading the individual status of the FEE boards, such as the voltage of the supplied power or temperature of the FPGA.

## C. Subdetector Frontend Electronics

Although the TTD and Belle2link are common, the requirements and hence the hardware designs for the FEE boards differ among subdetectors. The simplest example is the CDC FEE board, which does 48-channel preamplification, shaping and analog-to-digital conversion at a 31 MHz sampling cycle on the board, and time-to-digital conversion with a 1 ns least-significant-bit realized inside a Xilinx Virtex-5 FPGA. Other

subdetectors require additional preprocessing steps, typically using an external analog-to-digital conversion circuit and a digital logic built in another FPGA. The most complex FEE is the one for the TOP, which is built upon the Xilinx ZYNQ system-on-chip device with a Xilinx 7-series FPGA core and an Arm processor core which is used as a part of the pipeline to process the data. All subdetector frontend electronics are based on one of the Xilinx FPGA devices (Virtex-5, Spartan-6, Virtex-6, Kintex-7 or ZYNQ), with an exception of the flash-ADC controller board of SVD which uses the Stratix IV FPGA of Intel (Altera) [10].

## D. PXD and Backend

The data read out by the COPPER are collected and built into a raw event without the PXD data. The raw events are fed into one of the streams of the high level trigger (HLT) computing nodes, where the full event reconstruction is made to filter the events by up to a factor of 5. The number of HLT streams has been and will be increased in a staged way; HLT has been operated with 9 streams until summer 2020, and the stream 10 was added during summer shutdown.

The PXD data is not combined at this stage for two reasons. First, the data size, which is an order of magnitude larger than the sum of the rest, is beyond the limited bandwidth of the COPPER based unified readout system. Second, the PXD does not contribute to the HLT event filtering. Contrary, we use the reconstructed charged tracks at HLT to reduce the PXD data by an order of magnitude by only saving the region-of-interest subset, and make the final event building before saving the data into a storage device.

## III. OPERATION AND PERFORMANCE

The phase 3 operation of Belle II has started in March 2019, which is the final phase of the commissioning with all subdetectors and accelerator components. In 2019, it continued until July, and then after a summer break, resumed from October till December. The run in 2020 started in February and continued until July, and resumed in October to end in December.

### A. Operating Condition

When SuperKEKB and Belle II are operated, it continues for 24 hours of 7 days per week, except for the scheduled half-day accelerator maintenance every 2 weeks. The current priority is in improving the peak luminosity rather than maximizing the integrated luminosity. Until summer 2020, day time of weekdays are usually devoted to the accelerator studies, and night time and weekend are used for physics data taking.

In the current operation we set a limit in the beam current, in order to keep the beam background condition to be below the limit of the integrated dose to the photon detector of the TOP. As the result, the trigger rate is still far below the design. Typical level-1 trigger rate around the end of the latest run period was around 4 kHz, whereas the expected trigger rate is 10 kHz for the full luminosity and the design trigger rate of the system is 30 kHz.

The time for accelerator studies are used to operate the data acquisition system with 30kHz dummy random triggers with intervals of a pseudo Poisson distribution. Since high voltage power supplies are not applied to the subdetectors, threshold is lowered for CDC to generate data with a reasonable occupancy. This dummy trigger operation has been useful to keep updating the firmware and software to improve the performance and stability.

A summary of the operation and dead-time fraction in 2020 is given in Fig. 4, with an overall efficiency of 84.2%.

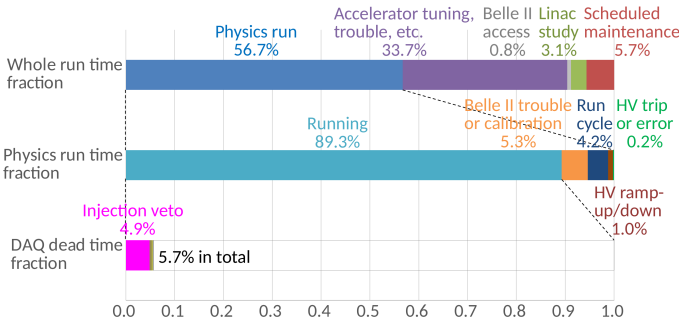


Fig. 4. Overall data acquisition efficiency in the run period from February to July, 2020.

### B. Dead-time Fraction

The largest dead-time fraction during the stable operation comes from the veto window after the beam injection. In the “continuous injection” mode, the linac injects the beam to the main ring during the run to keep the beam current and other accelerator conditions constant. The beam injection occurs at a cycle of 25 Hz at most. The level-1 trigger is entirely masked for a short period right after the injection timing, and then for the timing of the injected beam bunch for a longer period. The veto length is tuned to avoid spurious triggers due to the injection background, and in total about 5% of time is vetoed.

The second major dead time comes from the run restart cycle, which typically takes about 2.5 minutes, but may take longer depending on the situation. We pose an 8-hour limit for the run length, but most of the runs are stopped much earlier by the loss of the beam or by an error in the data acquisition.

The dead-time fraction from the data acquisition system is less than 1%. Two dominant contributions come from the trigger throttle and slow-down of the readout software somewhere in the chain, e.g. caused by a flood of log messages due to partially broken data. Otherwise the dead-time fraction due to the data acquisition system is negligibly small.

The trigger rate is still much lower than our design, but the background level is close to the highest level that detector can endure, as it is the largest limiting factor of the accelerator and detector operation. Hence the occupancy and the stress to the frontend electronics are rather severe, causing various kind of instabilities. Fig. 5 shows an example of the trigger rate of about 4kHz with several beam losses and troubles in a half day. Some of the problems are due to immaturity of the firmware which has been diligently improved as the

commissioning went on, while some are due to unstable hardware modules or connections which were replaced or fixed when it was possible.



Fig. 5. A typical half-day profile of the input (green, open histogram) and recorded (magenta, shaded) trigger rate, and data acquisition errors (vertical spikes). The drop and recovery of the input trigger rate corresponds to the loss of the beam and refill, while the lack of the output trigger rate corresponds to dead time due to an error.

### C. Readout Latency

We measure the latency of the data processing inside FEE as a part of the unified readout system, by including the timestamp of sending the data header into the data header itself. This can be then compared with the timestamp of the trigger in the data stream in an offline analysis.

Fig. 6 shows the estimated buffer occupancy at the COPPER using this data latency, assuming the the buffer is swiftly read out at the ideal bandwidth of the COPPER board. The event fragment stays inside the FIFO buffer until all data of four links are aligned. Therefore the occupancy illustrates the typical size of event fragments and variation of the processing time in the FEE.

We find the CDC data latency is the smallest and almost uniform, thanks to the single-board FEE configuration. We also find the TOP data latency is the largest and least uniform, as a result of software data processing in the Arm core of the FEE.

We also use this information to extrapolate to the 30 kHz design trigger rate to confirm that the COPPER buffer will not be overflowed.

## IV. PROBLEMS, TROUBLES AND SOLUTIONS

As already described, various troubles is one of the largest contribution to the inefficiency of data taking. Most of the troubles are understood and improved in 2020 with respect to the previous year, and will be further improved in coming runs. Here we classify the problems and troubles into four categories: single event upset (SEU), link errors, hardware failures and other troubles.

### A. Single Event Upset (SEU)

The FEE boards of CDC, TOP and ARICH are inside the detector and are expected to suffer from gamma rays and neutrons. According to the previous studies [11], the most affected part of a typical FEE board is the optical transceiver which is permanently damaged by a large dose of gamma rays and the FPGA whose configuration or data memory bit is flipped by SEU caused by neutrons.

The CDC uses the Xilinx SEU mitigation logic to correct the configuration memory altered by SEU. Successful SEU correction occurs a few times a day without affecting the

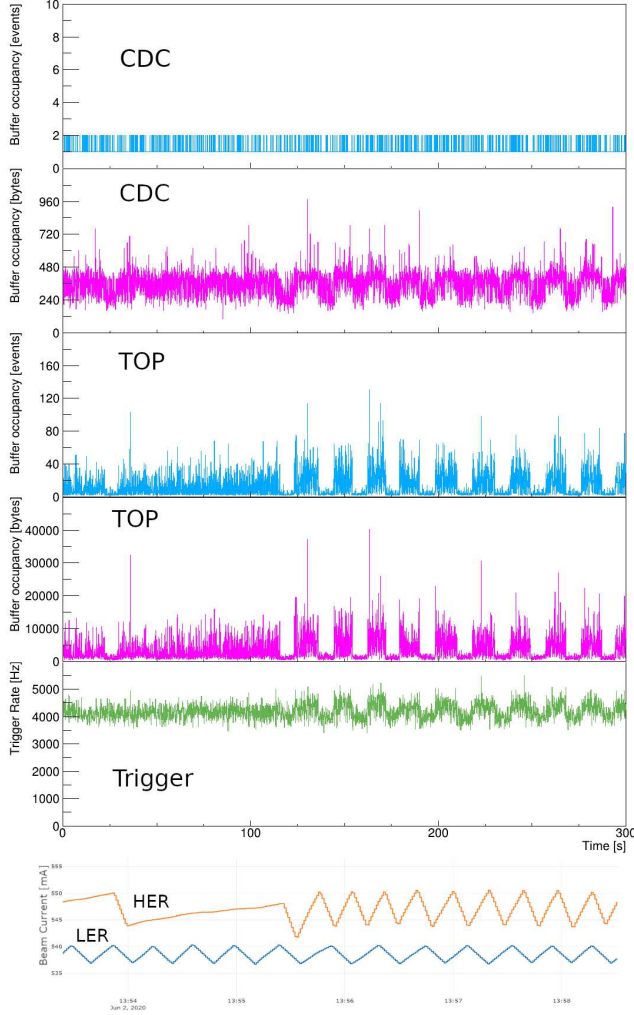


Fig. 6. Estimated buffer occupancy in terms of number of events and amount of bytes per link for CDC and TOP as a function of time from the beginning of a run (shown for the first 5 minutes). Pattern of quiet and busy time structure with a few spikes, corresponding to the continuous injection time structure and background spikes, are observed.

data acquisition, and it is monitored through the TTD system. However, the SEU mitigation code is not able to correct multiple bit errors at a time or errors in the mitigation code itself. It does not correct the data memory either, including those used as a part of state machines. These unrecoverable errors occurred at an average rate of once per day, of which those detected by the SEU mitigation logic is about 40%, as shown in Fig. 7. Then the FPGA has to be reprogrammed; the reprogramming takes less than 10s, but the detection and identification procedure of the error currently takes a much longer time.

The TOP also uses the SEU mitigation logic from Xilinx, and the ARICH uses a custom SEU mitigation logic [12] which has a superior performance compared with the one provided by Xilinx for the Spartan-6 FPGA.

Reduction of the down time is foreseen by automating the reprogramming procedure of the unrecoverable FPGA.

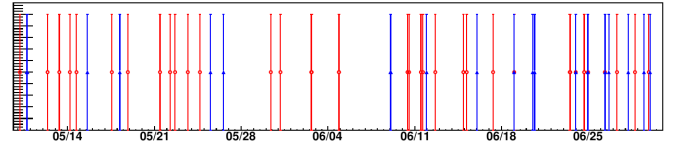


Fig. 7. History of unrecoverable SEU errors of CDC over 50 days detected by the mitigation logic (blue, triangle) and detected by data corruption (red, circle).

### B. Link Errors

Both of two custom protocols, b2tt and Belle2link, use predefined 8b10b control symbols to define the protocol and have an embedded data error checking mechanism using a cyclic redundancy check (CRC). An incorrect control symbol and a CRC error are identified as a link error, and propagated to the TTD system to stop the run. The link error, either in b2tt or Belle2link, has been so far the most frequent cause that stopped data taking. The error often repeated from the same link, caused by a particular version of firmware which happened to be less timing critical, on the line that has a smaller margin. Unstable FEE boards and cables were replaced to avoid the weak links during the shutdown period to make the entire system more stable.

We have made an investigation of the electric characteristics of the signal running on the CAT7 cables from the FTSW to the FEE during the summer shutdown period of 2020. We identified two particular cases that were improved during summer, one for the KLM and the other for the CDC.

For the KLM, we find a large sine-wave noise of around 300 kHz on the category-7 cables. This was turned out to be due to the lack of a proper ground connection at the FEE, and the 20 m long category-7 cables between FTSW and FEE. We have moved the location of the FTSW modules by introducing new small VMEbus crates and making the cable length to 10 m, and installed a proper grounding connection at the FEE. Some of the LVDS drivers of the KLM FEE were damaged and replaced during the run in 2020; the improper ground connection is suspected to have induced a large current from an external noise to cause the damage.

The CDC FEE boards were not accessible during the summer shutdown of 2020, but the clock and serial signals were examined near the FTSW module. We found a combination of a lower FTSW driver amplitude and a higher current draw at the FEE in particular connections makes it less immune to the crosstalk from the serial-b2tt-encoded line to the clock line. The crosstalk causes a glitch in the clock and causes a data error in Belle2link, although the glitch is not large enough to cause an error in the phase lock loop (PLL). Mostly due to this problem, up to 10 out of 299 FEE boards were masked at the worst case. This problem was completely cured by adding a delay to the serial link to avoid the edge transition of the serial b2tt data near the clock edge timing as shown in Fig. 8. The delay is added inside the IODELAY function of the Virtex-5 FPGA and hence this solution was accomplished only by updating the FTSW firmware.

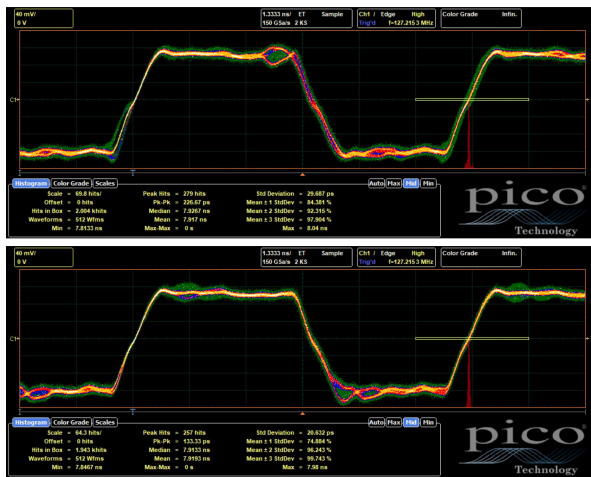


Fig. 8. Problematic clock signal with the edge affected by the crosstalk (top), and improved clock signal edge after adding a delay to the b2t serial signal (bottom).

### C. Hardware Failures, Other Troubles, and Prospects

The largest down time occurred during the run was due to the failure in one of the KLM FEE boards. This FEE was a data concentrator and could not be masked without losing a large fraction of data. The module had to be replaced by stopping the beam and accessing the detector area. Other hardware failure of the FEE boards for TOP and ARICH occurred inside the detector and they could not be replaced until the long shutdown period in 2022.

There were also down time due to the COPPER backend system, the HLT system, and slow control software problems.

The down time of the data acquisition system is one of the major concern of the future run period of Belle II. We have improved the the stability of the system in various ways at every major shutdown period and also during the run period. For the unavoidable errors such as the single event upset of the FEE, we are improving the monitor and error recovery procedure [13].

## V. CONCLUSIONS

We have presented the performance of the unified readout system of the Belle II experiment at the SuperKEKB  $e^+e^-$  collider during the first two years of the operation. We have been smoothly running at about 4 kHz level-1 trigger rate with a readout dead-time fraction below 1%. The largest dead time is from the unavoidable continuous injection veto, but a similarly large fraction of the dead time was caused by various errors in the unified readout system as well as in the rest of the data acquisition system. We have described the major problems we encountered, and solutions we found to improve the stability of the system and to reduce the dead time. We also confirmed using the real data that the unified readout system can handle the design level-1 trigger rate of 30 kHz. We expect a more stable operation with a higher luminosity and trigger rate in the coming runs.

## REFERENCES

- [1] T. Abe *et al.* (Belle II Collaboration), “Belle II Technical Design Report,” arXiv:1011.0352 [physics.ins-det].
- [2] K. Akai, K. Furukawa, H. Koiso *et al.* (SuperKEKB Collaboration), “SuperKEKB collider,” *Nucl. Instrum. Methods Phys. Res., Sect. A* vol. 907, pp. 188–199, Nov. 2018, 10.1016/j.nima.2018.08.017.
- [3] M. Nakao, T. Higuchi, R. Itoh, S.Y. Suzuki, “Data Acquisition System for Belle II,” *J. Instrum.*, vol. 5, C12004, Dec. 2010, 10.1088/1748-0221/5/12/C12004.
- [4] S. Yamada, R. Itoh, T. Konno, Z. Liu, M. Nakao, S. Y. Suzuki, J. Zhao, “Common Readout Subsystem for the Belle II Experiment and Its Performance Measurement,” *IEEE Trans. Nucl. Sci.*, vol. 64, pp. 1415–1419, Apr. 2017, 10.1109/TNS.2017.2693297.
- [5] M. Nakao, “Timing Distribution for the Belle II Data Acquisition System,” *J. Instrum.*, vol. 7, C01028, Jan. 2012, 10.1088/1748-0221/7/01/C01028.
- [6] VITA Standards, ANSI/VITA 1.0-1994. [Online] Available: <https://www.vita.com/Standards>.
- [7] Xilinx. [Online] Available: <https://www.xilinx.com/>.
- [8] “1149.7-2009 - IEEE Standard for Reduced-Pin and Enhanced-Functionality Test Access Port and Boundary-Scan Architecture,” Feb. 2010, 10.1109/IEEESTD.2010.5412866.
- [9] D. Sun, Z. Liu, J. Zhao, H. Xu, “Belle2Link: a Global data Readout and Transmission for Belle II Experiment at KEK,” *Phys. Procedia*, vol. 37, pp. 1933–1939, Oct. 2012, 10.1016/j.phpro.2012.01.036
- [10] Intel FPGAs and Programmable Devices. [Online] Available: <https://www.intel.com/content/www/us/en/products/programmable.html>
- [11] T. Higuchi, M. Nakao, E. Nakano, “Radiation Tolerance of Readout Electronics for Belle II,” *J. Instrum.*, 7, C01028, Feb. 2012, 10.1088/1748-0221/7/02/C02022.
- [12] R. Giordano, Y. Lai, S. Korpar, R. Pestotnik, A. Lozar, L. Šantelj, M. Shoji, S. Nishida, “Intermodular Configuration Scrubbing of On-detector FPGAs for the ARICH at Belle II,” 22nd Virtual IEEE Real Time Conference, Oct. 12–23, 2020.
- [13] T. Kunigo, A. Baur, M. Prim, S. Y. Suzuki, M. Nakao, R. Itoh, S. Yamada, Q.D. Zhou, R. Sugiura “Real-time monitoring of operational data in the Belle II experiment,” 22nd Virtual IEEE Real Time Conference, Oct. 12–23, 2020.